Journal of Hazardous Materials, 6(1982) 85—106
Elsevier Scientific Publishing Company, Amsterdam — Printed in The Netherlands

WIND-TUNNEL EXPERIMENTS ON DENSE GAS DISPERSION

ROBERT N. MERONEY

Fluid Mechanics and Wind Engineering Program, Civil Engineering Department, Colorado State University, Fort Collins, Colorado 80523 (U.S.A.)

(Received July 28, 1981; accepted November 9, 1981)

Summary

Laboratory simulation of negatively buoyant emissions into the earth's boundary layer is a valuable predictive tool to describe the motions of potentially hazardous chemicals such as propane, butane, chlorine, liquefied natural gas, freon, etc. In this paper are discussed some of the simulation criteria, special instrumentation, and results of wind-tunnel investigations of dense plume behavior. Such wind-tunnel data can be correlated in a manner that yields an empirical prediction of vapor dispersion from full-scale releases; nonetheless, certain facility and gas specific limitations must be recognized when interpreting an experimental program.

1.0 Introduction

Release of a dense gas from short stacks or near the ground is accompanied by initial descent and horizontal spreading caused by gravitational forces. Buoyancy forces tend to suppress advection by wind shear and dispersion by atmospheric turbulence. Such clouds will drift downwind from the source location at ground level, providing an opportunity for ignition if the gas is flammable or, perhaps, for acute toxic effects to life in its path. The mixing of such plumes is still only partially understood despite a significant research effort over many years [1—3]. The relative influence of gravity forces, viscous forces, entrainment at the plume front, entrainment at the upper surface, and modification of the background turbulent field due to stratification effects have been active subjects of discussion.

Dispersion in the atmospheric boundary layer can be simulated today in meteorological wind tunnels with sufficient accuracy to permit realistic scaling of dense gas escape hazards, pre-test planning for field experiments, and a post-test opportunity to extend the value of limited field measurements. Laboratory experiments permit a degree of control-of-safety, meteorological, and site variables not often feasible or economic at full-scale.

This paper considers the results of experiments performed in wind tunnels to examine the behavior of dense plumes during periods of gravity spread/air entrainment dominance. The special features which characterize dense gas dispersion and the associated similarity criteria are introduced. The behavior of elevated releases, surface releases, and dense gas plume interaction with surface obstructions are discussed in successive sections. Finally, sources of uncertainty and efforts to improve modelling procedures are presented.

2.0 Dense gas dispersion: General behavior

Dense gas plumes from elevated sources may result whenever the fractional density ratio, Δ, is greater than zero, i.e.

$$\Delta \cong 1.0 - \frac{28.9}{m_0}\left(\frac{T_0}{T} - 8\,\frac{\dot{M}_w}{\dot{M}_0}\right) \quad (1)$$

where T_0 is effluent temperature, m_0 is the mean molecular weight of the effluent, and $\dot{M}_w$ and $\dot{M}_0$ are the mass flux of liquid water and total mass flux of the effluent, respectively. If $\Delta > 0$ the plume is heavier than air. It may fall to the ground rather close to the source if the Froude number

$$Fr = \frac{u}{\sqrt{g\Delta d_0}} < C \quad (2)$$

where u is the reference wind speed, d_0 is the exit plume diameter, and C lies between 0.7 and 7.7 depending on surface roughness, wind speed and stratification condition. Prediction of the behavior of dense plumes is also often aggravated by the influence of surface interaction, heat transfer, latent heat release, and a transient character.

The effect of negative buoyancy on plume behavior and resulting downwind concentrations will be greatest when crosswinds are light, and turbulence intensities are low. The sinking velocity of the plume relative to the horizontal convective velocity will be much higher than under "normal" conditions. In such cases, the entrainment of outside air into the plume, and the resulting diffusion, is a function of this interaction between plume and crosswind and approaches the behavior of a turbulent plume injected into a laminar crosswind. When the density is sufficient to bring a plume to ground level, large lateral spreading occurs after touchdown.

A ground-level release of a dense gas is characterized by rapid slumping toward the surface. Horizontal dimensions increase rapidly with an associated decrease in vertical dimension until such time as entrainment is significant. The ratio of vertical height to crosswind dimension remains quite small over most times of interest. The initial potential energy of the dense gas is converted rapidly to kinetic energy; however, this energy is also transmitted to the surrounding ambient fluid and is dissipated by turbulence.

The tendency for dense gases to remain near the ground enhances the importance of plume interaction with surface features. Slight changes of surface slope on the presence of buildings, fences, or dikes will affect plume behavior. These features produce three-dimensional secondary motions or local areas of enhanced turbulence; hence, laboratory models are often required to adequately predict dense gas dispersion.

3.0 Physical modelling criteria

Two systems at different geometric scales will exhibit similar behavior if geometric, kinematic, dynamic, and thermic similarity are guaranteed by the equality of all pertinent ratios of forces, boundary conditions, and initial conditions [4]. When it is not possible to obtain a rigorous similarity in all variables, it is necessary to neglect some contributors or phenomena; hence partial similarity. This is permissible when the contributions of such terms are small or their absence conservative.

3.1 Simulation of the atmospheric surface layer

The atmospheric boundary layer is that portion of the atmosphere extending from ground level to approximately 600 meters within which the major exchanges of mass, momentum, and heat occur. Physical modelling in wind tunnels requires consideration of the physics of the atmospheric surface layer as well as the dynamics of plume motion. The reliability of wind-tunnel shear layers for modelling atmospheric shear layers has been demonstrated by many investigators [5]; hence only special aspects associated with dense gas dispersion need be discussed here.

The major practical limitations of accurate wind-tunnel simulation of dense gas dispersion are operational constraints. These include, particularly, the inability to obtain a steady wind profile, the accurate simulation of atmospheric turbulence at the lowest wind speeds of interest, and Reynolds number constraints (as yet somewhat ill-defined) associated with the proper scaling of near-field turbulence. When combined with estimates of the restraint of plume expansion by the tunnel sidewalls, these considerations permit the development of a performance envelope for a particular wind-tunnel facility, examples of which are given by Meroney et al. [6,7].

3.2 Simulation of dense gas dispersion

There exist in the literature descriptions of a variety of different wind-tunnel studies on the dispersion of neutral gas plumes in the atmosphere [8—13]. These referenced studies are significant in that simulation was confirmed by direct prototype measurements. Successful simulations exist for isolated plume behavior [8], as well as plume perturbation situations caused by buildings [9,10,11], topography [12,13] and stratification [8,11,12,13].

When one considers the dynamics of gaseous plume behavior, exact similitude requires the simultaneous equivalence of mass, momentum and volume flux ratios, densimetric Froude number, Reynolds number, and specific gravity. Consideration of variable property, non-ideal gas, and thermal behavior of the plume mixture introduce additional constraints on specific heat capacity variations [14].

Previous experiments by Hoot and Meroney, Bodurtha, Van Ulden, and Boyle and Kneebone have confirmed that the Froude number is the parameter which governs plume spread rate, trajectory, plume size and entrainment when gases remain negatively buoyant during their entire trajectory [15,16, 17,18]. In the case of spills of liquefied inflammable gases like LNG and LPG, buoyancy of the plume will be a function of both mole fraction of the gas and temperature. Thus, depending upon the relative rate of entrainment of ambient gases versus rate of thermal transport from surrounding surfaces, the state of buoyancy may vary from negative to positive. Earlier measurements for cold gas releases now suggest that heat transfer effects may be small over the significant time scales associated with non-calm situations (i.e. $U_p > 1$ m/sec); hence gas density should be adequately simulated by isothermal high molecular weight gas mixtures. This agrees with the result independently reported by Boyle and Kneebone that room temperature propane simulated an actual LNG spill quite well [18].

The Reynolds number cannot be made equal for model and prototype for scales ranging from 1:100 to 1:600. Fortunately, equality is not required if the magnitude and quality of the shear laver turbulence is similar to the full-scale — hence the use of specially designed meteorological wind-tunnels [5]. It is possible to obtain full-scale values of the remaining non-dimensional parameters by reducing the reference velocity to very low values (of the order of 0.2 m/sec to simulate a 3 m/sec full-scale wind) and increasing the atmospheric temperature difference as necessary. In some cases, investigators modify the density ratio $(\rho_a - \rho)/\rho_a$ to permit the use of larger and more convenient values of model velocity. Unfortunately, this also modifies inertial effects, time scale ratios, and volume dilution rates.

A reasonably complete simulation may be obtained in some situations even when a modified initial specific gravity is stipulated. By increasing the specific gravity of the model gas compared to the prototype gas, one increases the reference velocity over the model. It is difficult to generate a flow which is similar to that of the atmospheric boundary layer in a wind tunnel run at very low wind speeds. Thus the effect of modifying the model's specific gravity extends the range of flow situations which can be modelled accurately. Isyumov and Tanaka [19] found that Froude number and volume flux equality provided conservative ground-level concentrations for buoyant plumes. Skinner and Ludwig [20] and Kothari and Meroney [21] obtained similar plume trajectories when flux, Froude number and momentum ratio equivalence are required.

4.0 Elevated emissions of dense gases

Dense gases descending from elevated sources have been reported by several observers. Scorer reports cases of two power plants emitting wet-washed plumes with apparently insufficient elimination of free water, in which the subsequent evaporation of the free water cools the plume and causes it to sink [22]. Bodurtha observed descent of dense gases from chemical industry relief valves [16]. The exit stack for the National Transonic Wind Tunnel facility at Langley Research Center, NASA, will omit large quantities of cold nitrogen—air mixtures which produce ground fog under certain operational and meteorological conditions [21].

Bodurtha conducted wind-tunnel tests of emissions of freon—air mixtures into a crosswind. Various combinations of density, exit velocity, crosswind velocity and stack diameter were used in obtaining smoke pictures. The results were correlated by an expression for the maximum rise height:

$$H = 5.44\, D_0^{0.5}\, R^{0.75} \tag{3}$$

in which H is the maximum rise height of the plume centerline in feet, D_0 is the stack diameter in feet, and R is the ratio of the exit velocity to the wind speed. This formula has the disadvantage of being dimensionally inhomogeneous, and the absence of relative density terms makes its application questionable as the specific gravity approaches unity.

Hoot and Meroney examined dense vertical plumes in a quiescent medium, and dense plumes injected into both laminar and turbulent crosswinds [15]. The vertical plumes emitted into a quiescent atmosphere were observed to rise initially in a jet with almost linear growth of radius with vertical distance. This jet region appeared to encompass from 1/4 to 1/3 of the total rise height. The dense vertical plume appears to re-entrain some of the falling dense fluid, so that the flux of negative buoyancy increases with distance, rather than being constant. The point of maximum rise of the plume correlates as

$$\frac{\Delta h}{d_0} = 2.96\, F_R\,, \text{ where}$$
$$F_R = \frac{\sqrt{\rho_0} w_0}{\sqrt{(\rho_0 - \rho_a) g d_0}} \tag{4}$$

where d_0 is stack diameter, w_0 is exit velocity, and ρ_0 is exit density.

Plumes injected vertically into a crosswind initially lofted to some maximum height, subsequently descended to the ground, impacted with nearly a circular cross-sectional configuration, but then spread laterally as they dispersed downwind (see Fig. 1). Hoot and Meroney tuned an integral equation analytical plume theory with wind-tunnel experiments to estimate downwind surface concentrations. The components of the analysis required one to first estimate plume rise, Δh, as

$$\frac{\Delta h}{d_0} = 1.32\, (SG)^{2/3} (F_{RH})^{2/3} (R)\,, \tag{5}$$

where $SG = \rho_0/\rho_a$

$R = w_0/u$, and

$F_{RH} = u/\sqrt{g(SG-1.0)d_0}$; and

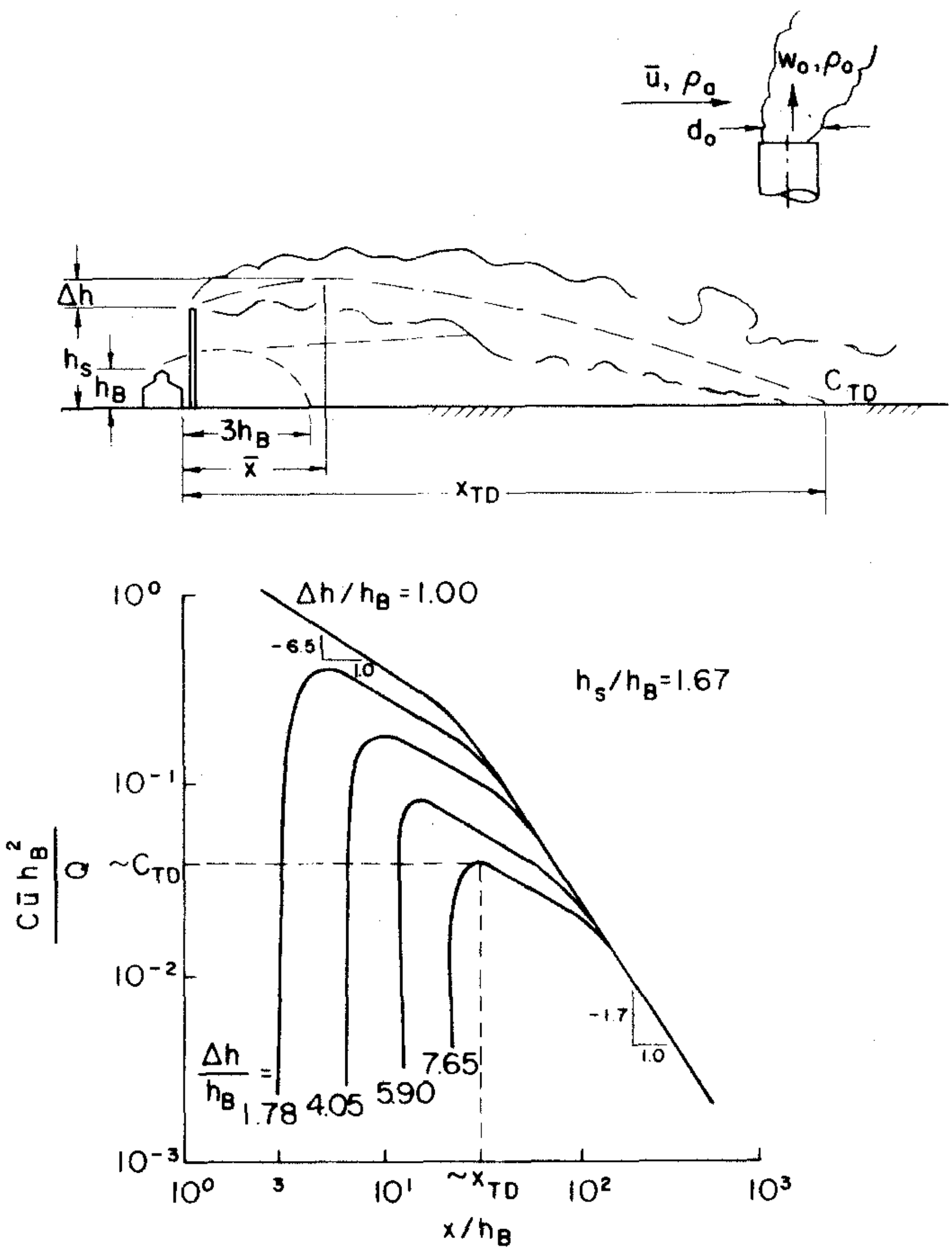

Fig. 1. Dispersion of dense plumes from short stacks, Hoot and Meroney [15].

downwind distance to maximum plume rise, $\bar{x}$, as

$$\frac{\bar{x}}{d_0} = (SG)\,(F_{\mathrm{RH}})^2\,(R)\,. \tag{6}$$

Touchdown distance, x_{TD}, may be evaluated from

$$\frac{x_{\mathrm{TD}} - \bar{x}}{d_0} = 0.56 \left[\frac{\left(\frac{h_s}{d_0}\right) + 2\left(\frac{\Delta h}{d_0}\right)^3 - \left(\frac{\Delta h}{d_0}\right)^3}{R} \right]^{1/2} F_{\mathrm{RH}}\,. \tag{7}$$

Symbols are defined in Fig. 1.

Note that as $u \to 0$, $F_{\mathrm{RH}} \to 0$, $\bar{x} \to 0$, $\Delta h \to 0$ and $x_{\mathrm{TD}}/h_s \to 3\,F_{\mathrm{RH}}$. The constant, 3, compares well to the value 4.5 proposed by Briggs based on Bodurtha's visualization experiments.

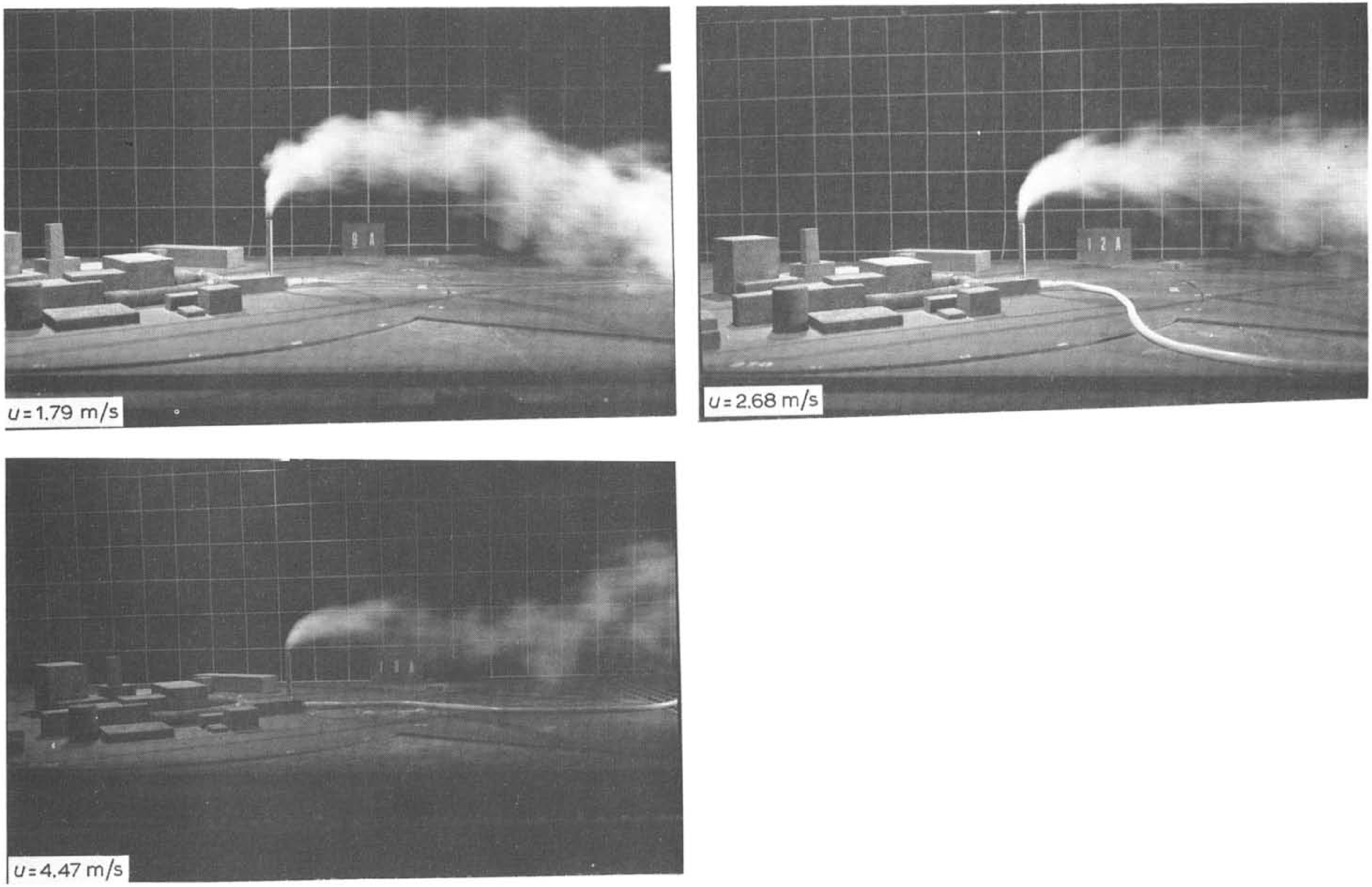

Fig. 2. Behavior of a cold dense gas plume emitted from model National Transonic Facility Exhaust Stack, model Scale 200:1, Kothari and Meroney (1979) [21].

At touchdown the surface concentrations, C_{TD}, are of the order

$$K_c \equiv \frac{C_{TD} u d_0^2}{Q} \simeq 3.10 \left(\frac{2\Delta h + h_s}{2d_0}\right) - 2 . \tag{8}$$

Concentrations decrease from their touchdown values at a negative 0.65 power of distance, x, until the curve intercepts the −1.7 slope behavior of a ground source as shown in Fig. 1.

Kothari and Meroney examined the behavior of a dense plume consisting of a breathable mixture of cold nitrogen and oxygen emitted from a 1:200 scale model of the National Transonic Facility exhaust stack at NASA, Langley. In this case the dense gases not only descended but interacted with local buildings as shown in Fig. 2. Nonetheless, measurements made with and without buildings present suggested only second-order aerodynamic effects, so results are compared to the predictive relations suggested by Hoot and Meroney in Table 1. The results are nearly equivalent, except for the plume trajectory for the case of 1.8 m/sec wind and exhaust velocity of 23 m/sec. Streamline deflection by the NTF building is the likely explanation for this deviation.

5.0 Surface emissions of dense gases

A number of laboratory experiments have been performed to evaluate the influence of plume density on ground-level gaseous plume dispersion. Sakagami and Kato (1968) [39] measured diffusion and vapor rise from a small 5 × 10 cm LNG well in the floor of a 50 × 50 cm cross-section × 200 cm length wind-tunnel. They confirmed a tendency for the gas to remain concentrated at ground level. Boyle and Kneebone [18] released LNG on water, pre-cooled methane, and propane in a specially built 1.5 × 1.2 m cross-section by 5 m long asbestos-wall wind-tunnel. No attempt was made to scale the atmospheric surface layer velocity profile or turbulence. They concluded that room-temperature propane simulated an LNG spill quite well, but the pre-cooled methane runs lofted suggesting to the authors incorrect release temperature or exaggerated heat transfer from the ground surface.

5.1 Point and area sources of dense gases

Hoot and Meroney, Hall et al., and Meroney et al., have considered the behavior of continuous ground-level point sources of heavy gases in wind tunnels [15,23,24,25]. The principle characteristic of such plumes is their very wide, shallow nature. In general, the plume size reduces rapidly with increasing wind speed, but it still retains a low, flat form with significant upwind and lateral travel. At higher wind speeds the plume upper boundary becomes more turbulent and unsteady, resulting in rapid vertical growth as local Richardson numbers decrease. Visualization tests performed over a simple ground-level area source revealed that the plumes' upwind spread, L_U,

TABLE 1

Comparison of NTF model plume characteristics with that predicted by Hoot and Meroney [15]

w_0 (m/sec)	u (m/sec) at 10 m height	Downwind distance to maximum plume rise, $\bar{x}$ (m)		Touchdown distance of plume center, x_{TD} (m)		Plume rise Δh (m)		K_c (maximum)	
		Calculated	Experimental	Calculated	Experimental	Calculated	Experimental	Calculated	Experimental
23	1.8	32	65	156	240	45	46	0.26	–
23	2.7	49	45	255	250	39	41	0.32	–
23	22	–	–	–	–	–	–	0.80	0.46*
46	1.8	63	70	255	325	89	75	0.09	–
46	2.7	98	90	410	330	77	70	0.11	–

*Wind direction = 180° and maximum measured value with NTF complex.
All other experimental data are for wind direction = 0°.

and lateral spread at source center, L_{H_0}, correlate with the buoyancy length scale, $l_b = Qg(SG-1)/u^3$, for a wide range of source and shear flow conditions [25] (see Fig. 3). Britter reported similar results for dense salt plumes emitted in a water flume and liquefied natural gas (LNG) plumes developing downwind of sea spills [26]. Specific gravity ratios considered ranged from 1.0 to 4.2 and lateral scales from 1.0 to 500 meters.

Along the plume centerline, gas concentrations fall off rapidly with increasing windspeed. Although density differences were observed to have a significant effect on downstream diffusion pattern, the effect on centerline concentrations appear primarily multiplicative. Hoot and Meroney studied point source ground releases in both neutral and stably stratified turbulent boundary layers [15]. They found that varying specific gravity of the source gas from 1.0 to 3.0 increased maximum ground concentrations by no more than 40%, while decay rates of concentration with distance remained the same.

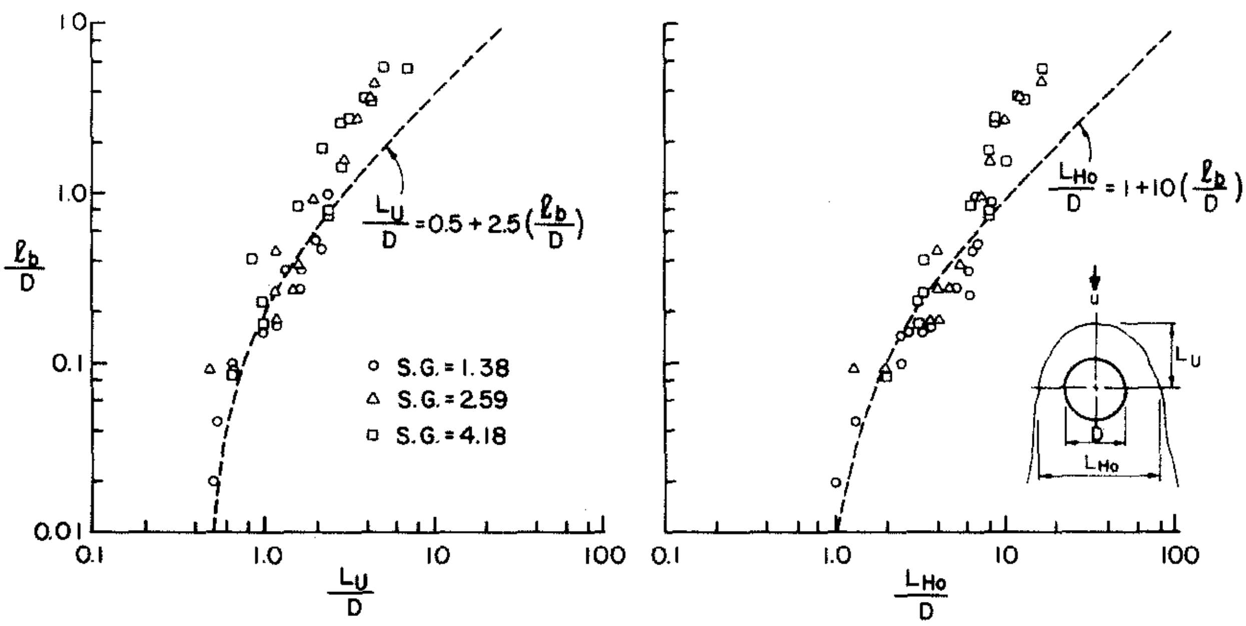

Fig. 3. Spreading characteristics of dense gas area sources: Upstream travel distances and lateral tunnel distances, Meroney et al. (1980) [25].

5.2 Volume sources and short-term releases of dense gases

Short-term or instantaneous releases of dense gas may occur during explosions or boil-off of gases from limited spills of liquefied gases such as ammonia or LNG. Meroney et al. released carbon dioxide in a 1:106 scale model simulation of test 044 from the Capistrano land spill field test series supported by the American Gas Association [27]. This test involved a spill of LNG into a 24.4 m diameter area surrounded by a 46 cm high dike. Figure 4 compares concentration sensor response at equivalent locations from the model and field measurements. The wind-tunnel simulation did not reproduce the large and intermittent concentration peaks at late times as observed in the field; however, it is believed that these perturbations may be due to gustiness, changes in wind direction, and cracking of the field test dike floor which produced spikes in the late boil-off rate.

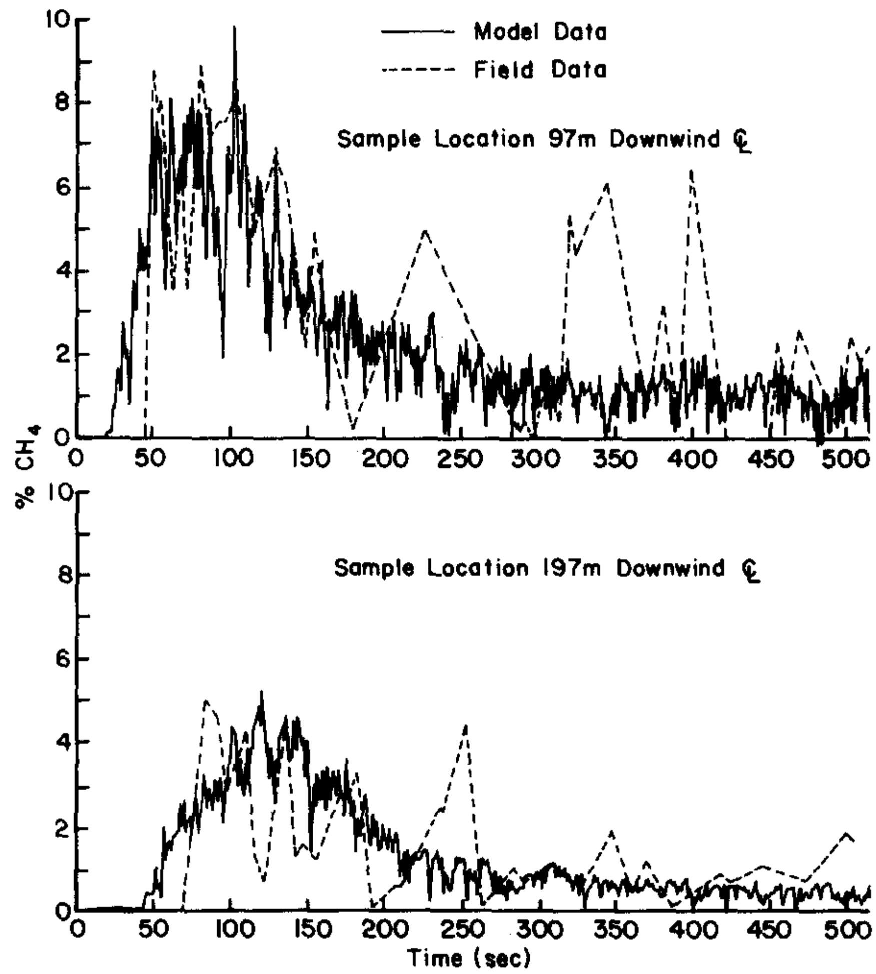

Fig. 4. Comparison of wind tunnel and field data for the Capistrano 044 LNG Land Spill Experiments [27]: Wind speed 5.4 m/sec, Stability category D-C, Wind tunnel scale ratio 106:1.

Hall has compared data from short time releases of BCF gas in a wind-tunnel shear layer with Trial 33 from the Porton Field releases of freon mixtures [24,28]. Situations from the two sets of data existed which had equal modified Froude numbers. The scale of the model test was 1: 34.2 based on the volume of gas released. Wind speeds were determined at a scaled reference height. As noted in Fig. 5, the level of agreement between wind-tunnel model and field trial seems good. The peak concentrations, the form of concentration distribution with time, and the plume arrival and departure times all match quite well when one considers that these field tests are separate realizations from some probability distribution about an ensemble behavior. Hall has also prepared figures based on laboratory experience which predict downwind hazard limits for propane or butane escape [24].

During a 5 m^3 LNG spill series onto a water basin at the Naval Weapons Center at China Lake, California, concentrations were measured at up to eight locations downwind [29]. Meroney and Neff replicated the meteorological, topography, and spill conditions to a scale of 1: 85 for the four field tests [30]. Correlation of results ranged from poor to very good, probably because fluctuation present during the field tests were as large as $\pm 50°$ in wind direction and ± 1.8 m/sec in wind speed. During field test LNG-21 wind conditions were more stationary, and Fig. 6 displays good agreement between laboratory and field measured peak concentrations.

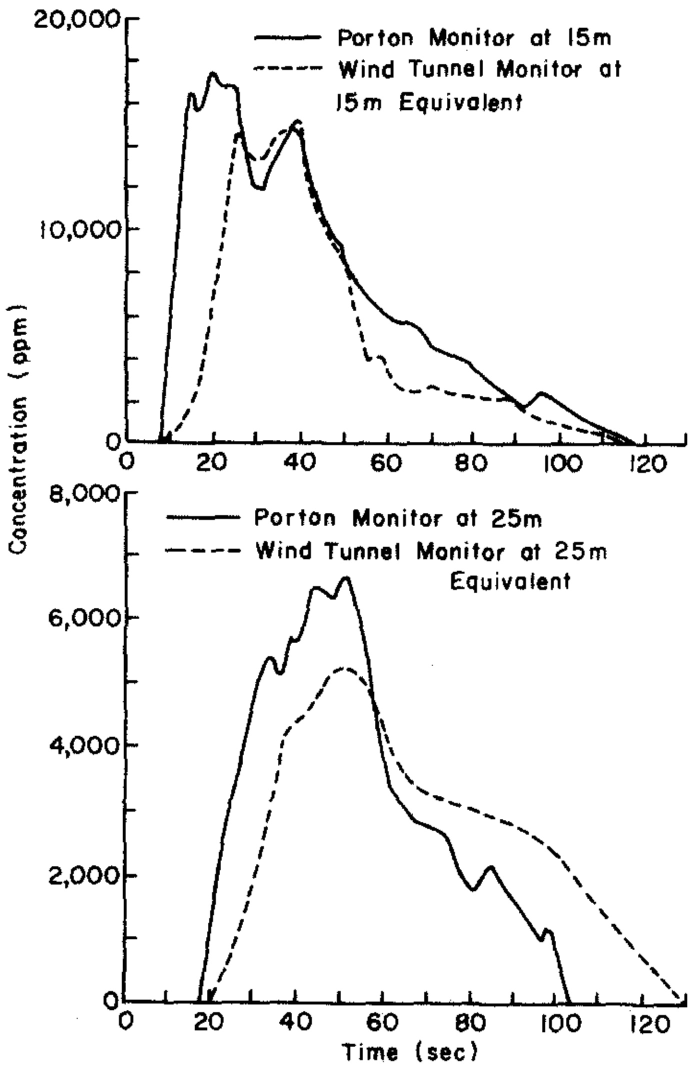

Fig. 5. Comparison of wind tunnel and field data for Porton Field Test Trial No. 33: Wind speed 1.0 m/sec, Source gas specific gravity = 2.2, Stability category B-C; Wind-tunnel scale 34.2 :1.

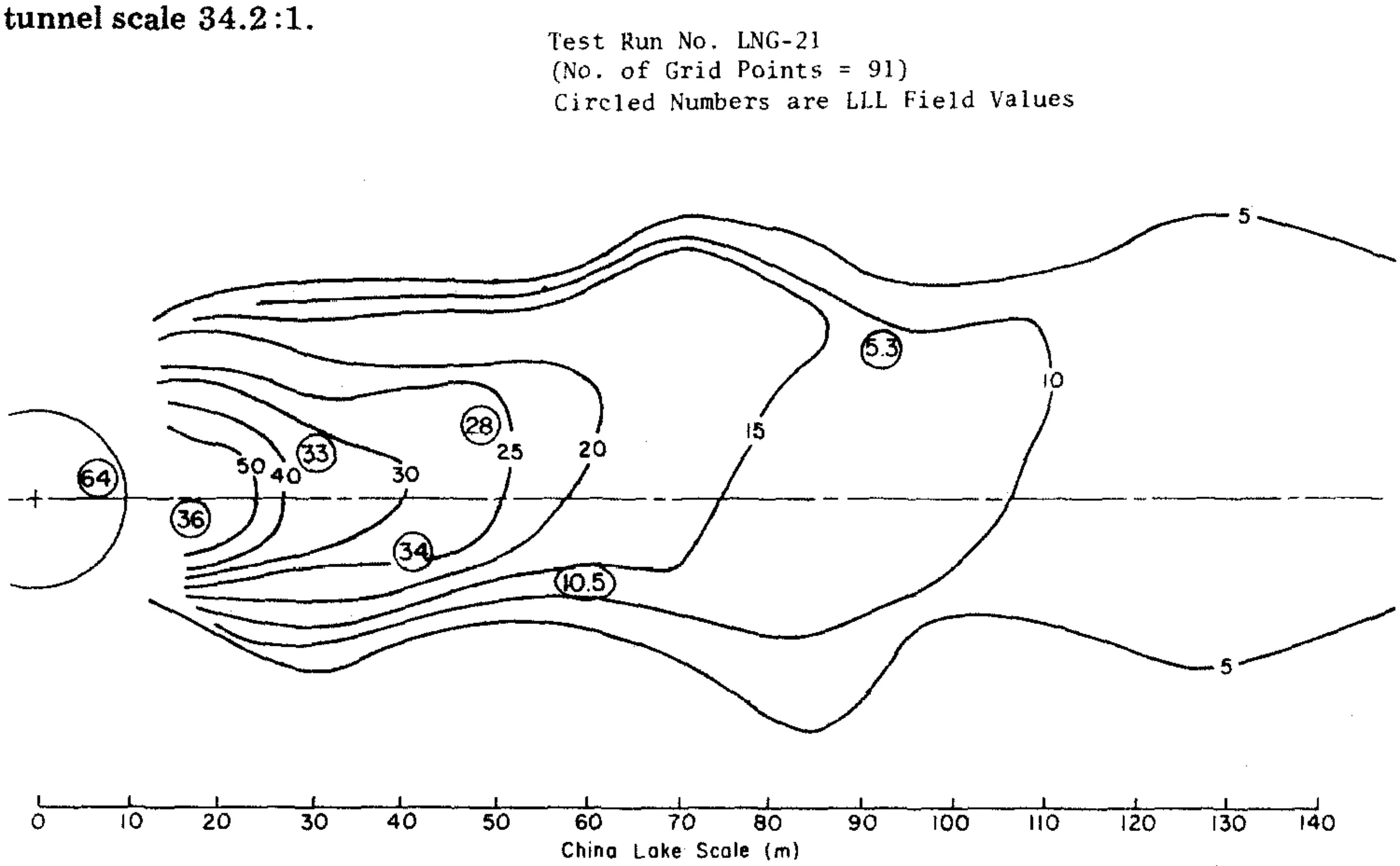

Fig. 6. Comparison of wind tunnel and field data for the six cubic meter LNG spill test No. LNG-21 at China Lake Naval Weapons Test Center, Neff and Meroney [14]: Wind speed 4.9 m/sec, Stability category C; Wind-tunnel scale ratio 85 :1.

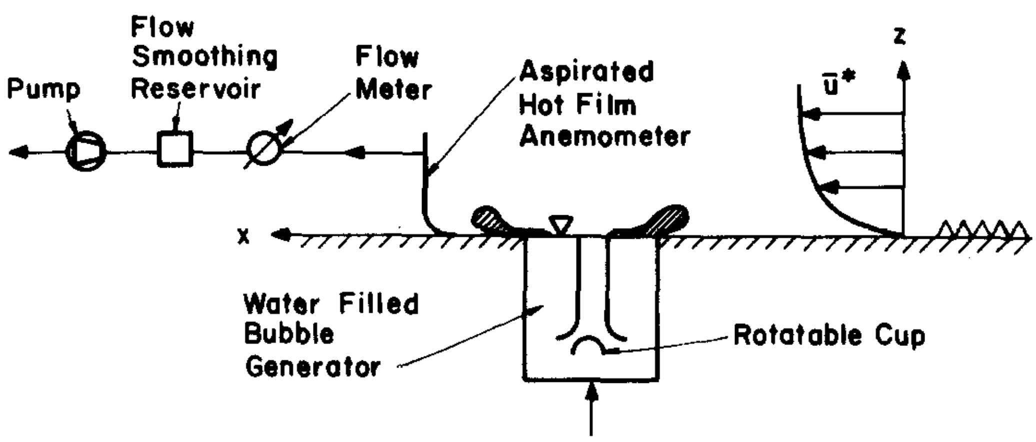

Fig. 7. Experimental configuration for release of instantaneous volume sources of dense gas, Lohmeyer et al. [31].

A sudden release of a volume of dense gas near the ground is characterized by a slumping of the volume toward the ground, followed by a radial expansion preceded by a gravity current head. Wind-tunnel model experiments with releases of dense gas volumes of 50 cm^3 reproduced dense plume behavior previously seen in field experiments at scales up to 350 times greater [31]. Lohmeyer et al. used a special source volume generator to quickly release measured volumes of Freon-12 gas (specific gravity = 4.17) at a wind-tunnel floor (Fig. 7). A fast response katherometer system measured time-dependent concentration variation. Measurements were compared with a modified version of the generalized box model for dense gases proposed by Fay [32]. In a calm environment the radial variation of plume dilution, V_{initial}/V, versus dimensionless radius, $R^* = R/V_{\text{initial}}^{1/3}$, is shown in Fig. 8. These measurements support the notion that the radial spreading speed is independent of dilution and directly proportional to the local excess hydrostatic head within the cloud, i.e.

$$dR/dt = \alpha(g'H)^{1/2} \tag{9}$$

where α is equal to unity; and that the entrainment velocities at the surface of the cloud are also proportional to excess hydrostatic head, i.e.

$$u_z = c_z(g'H)^{1/2}, \quad u_r = c_r\,(g'H)^{1/2} \tag{10}$$

and

$c_r \simeq c_z \simeq 0.10.$

These measurements agree with those discussed by Simpson and Britter and Germeles and Drake [33,34].

Wind shear superimposed over volume releases of dense gas initially displace higher concentrations further downwind with increasing wind speed. As shear flow mixing increases it begins to dominate over inertial/buoyancy entrainment mechanisms, hence at very high velocities the maximum peak concentrations retreat back towards the source. As velocities increase further, the gravity dominated portion of the plume lifetime decreases until dispersion is essentially passive. Most of the data taken by Hall was for high wind speed

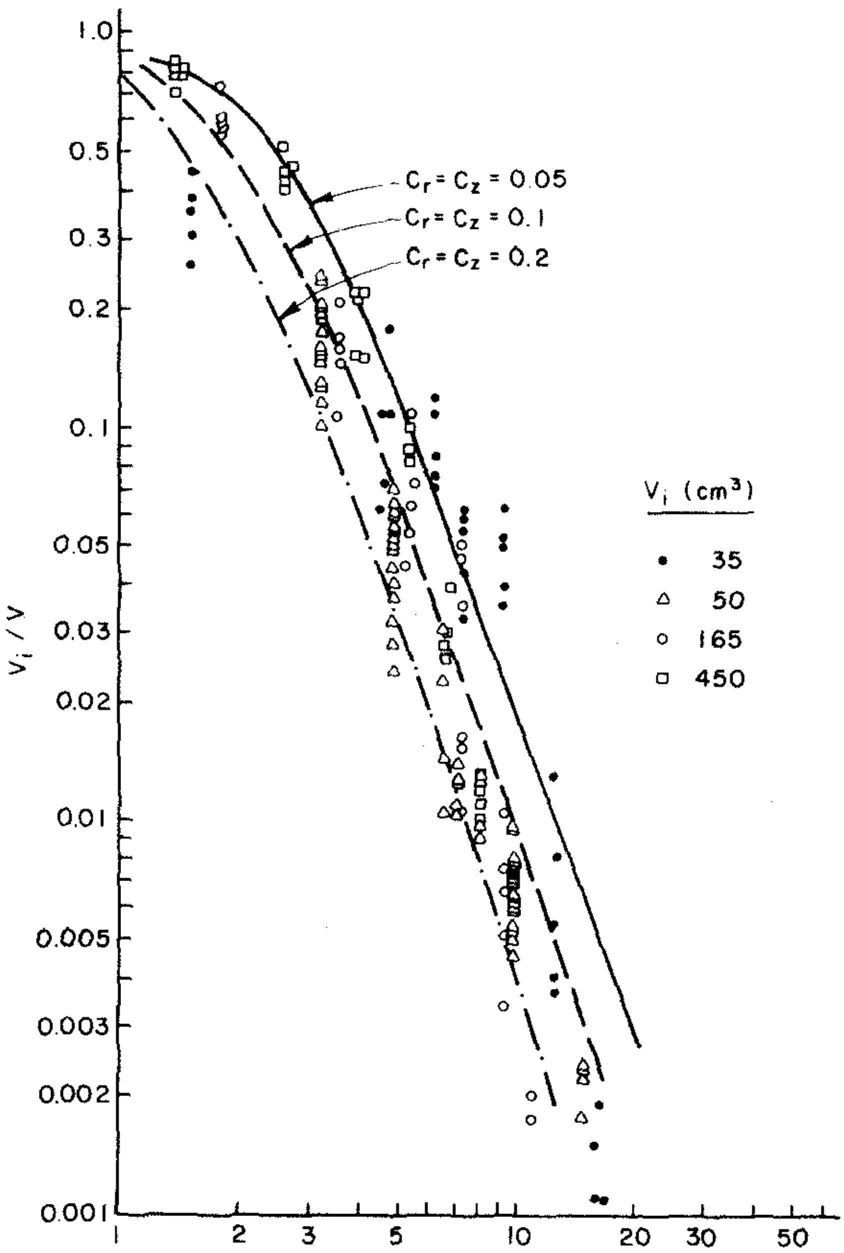

Fig. 8. Plume dilution, V_i/V, versus Dimensionless Radius, $R^* = r/V^{1/3}$, $U_L^* = 0$, Lohmeyer et al. [31].

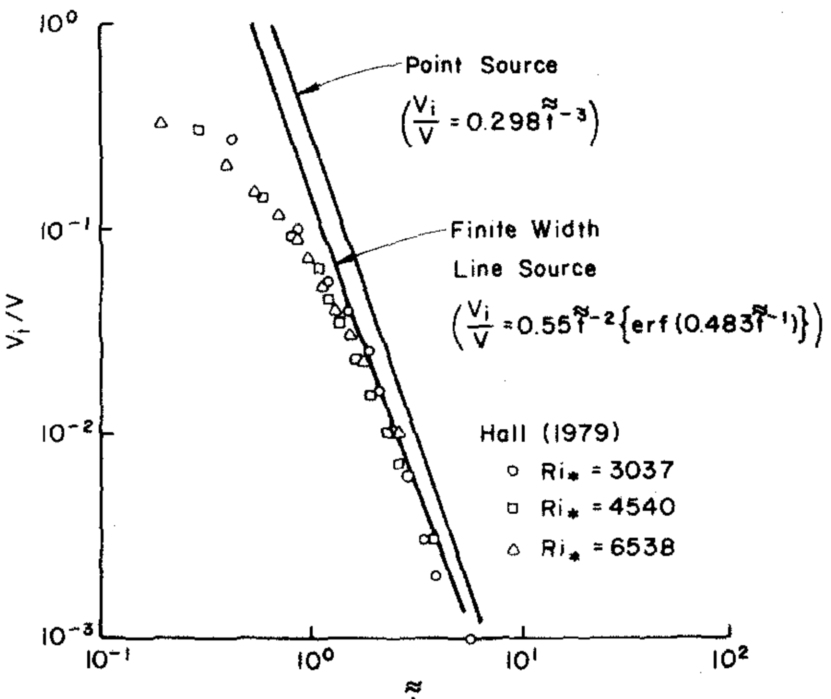

Fig. 9. Asymptotic dilution of short-term releases of dense gases: Comparison of Lagrangian similarity solution for passive sources, Yang and Meroney [35] with Dense Gas Tests, Hall (1979) [24].

or low modified Froude number conditions [24]. Figure 9 indicates that plume concentrations decay with time to a power of −3. Also shown are predictive lines for instantaneous point and finite width sources from Lagrangian similarity theory proposed by Yang and Meroney [35]. A ground-level neutrally buoyant point source will decay as

$$\left(\frac{V_i}{V}\right)_{max} = 0.298\,\tilde{\tilde{t}}^{\,-3} \quad \text{where}$$

$$\tilde{\tilde{t}} = \frac{t^*}{R_i^{1/2}} = \frac{t\,u}{V_i^{1/3}}, \tag{11}$$

and a line source of width dimension equal to $2\,V_i^{1/3}$ will decay as

$$\left(\frac{V_i}{V}\right)_{max} = (0.55/\tilde{\tilde{t}})^2\,[\mathrm{erf}\,(0.483/\tilde{\tilde{t}})]. \tag{12}$$

Although some of Hall's releases were extended over considerable time, all data asymptotically approach the passive gas dispersion theory.

5.3 Dense cold gases versus dense isothermal gases

Exact variation of the density ratio for the entire life of a model plume is difficult to simulate for plumes which simultaneously vary in molecular weight and temperature. To emphasize this point more clearly, consider the mixing of two volumes of gas, one being the source gas, V_s, the other being ambient air, V_a. Consideration of the conservation of mass and energy for this system yields*

$$\frac{\rho_g}{\rho_a} = \frac{\left(\frac{\rho_s}{\rho_a} V_s + V_a\right)}{\left(\frac{T_a}{T_s} V_s + V_a\right)\left(\frac{C_{p_s} M_s}{C_{p_a} M_a} V_s + V_a\right)\left(\frac{C_{p_s} M_s}{C_{p_a} M_a}\frac{T_a}{T_s} V_s + V_a\right)}$$

If the temperature of the air, T_a, equals the temperature of the source gases, T_s, or if the product of the specific heat capacity and molecular weight, $C_p M$, is equal for both source gas and air then the equation reduces to:

$$\frac{\rho_g}{\rho_a} = \frac{\frac{\rho_s}{\rho_a} V_s + V_a}{V_s + V_a}.$$

*The pertinent assumption in this derivation is that the gases are ideal and properties are constant.

Thus for two prototype cases: (1) an isothermal plume and (2) a thermal plume which is composed mostly of air, it does not matter how one produces the model density ratio as long as the initial density ratio value is equal for both model and prototype.

For a plume whose temperature, molecular weight, and specific heat are all different from that of the ambient air, i.e. a cold natural gas plume, equality in the variation of the density ratio upon mixing must be relaxed slightly if one is to model utilizing a gas different from that of the prototype. In most situations this deviation from exact similarity is very small.

Scaling of the effects of heat transfer by conduction, convection, radiation, or latent heat release from entrained water vapor cannot be reproduced when the model source gas and environment are isothermal. Fortunately, in a large majority of industrial plumes the effects of heat transfer by conduction, convection, and radiation from the environment are small enough that the plume buoyancy essentially remains unchanged. The influence of latent heat release by moisture upon the plume's buoyancy is a function of the quantity of water vapor present in the plume and the humidity of the ambient atmosphere. Such phase change effects on plume buoyancy can be very pronounced in some prototype situations. Humidity effects are expected to reduce the extent in space and time of plume buoyancy dominance on plume motion. Hence a dry adiabatic model condition should be conservative.

The influence of heat transfer on cold dense gas dispersion due to cryogenic liquid spills can be divided into two phases. First, the temperature (and hence specific gravity) of the plume at exit from a containment tank or dike is dependent on the thermal diffusivity of the tank—dike—spill surface materials, the volume of the tank—dike structure, the actual boil-off rate, and details of the spill surface geometry. A second plume phase involves the heat transfer from the ground surface beyond the spill area which lowers plume density.

It is tempting to try to simulate the entire transient spill phenomenon in the laboratory, including spill of cryogenic fluid into the dike, heat transfer from the tank and dike materials to the cryogenic fluid, phase change of the liquid and subsequent dispersal of cold gas downwind. Unfortunately, the different scaling laws for the conduction and convection suggest that markedly different time scales occur for the various component processes as the scale changes. Since the volume of dike material storing sensible heat scales versus the cube of the length scale, whereas the pertinent surface area scales as the square of the length scale, one perceives that heat is transferred to a model cold plume much too rapidly within the model containment structures. This effect is apparently unavoidable since a material having a thermal diffusivity low enough to compensate for this effect does not appear to exist. When calculations for the full-scale situation suggest minimal heating of a cold gas plume by the tank—dike structure, it may suffice to cool the model tank—dike walls to reduce the heat transfer to a cold model vapor and study the resultant cold plume.

Boyle and Kneebone released, under equivalent conditions, room temperature propane and LNG onto a water surface. The density of propane at ambient temperatures and methane at −161°C relative to air are the same [18]. Using the modified Froude number as a model law they concluded dispersion characteristics were equivalent within experimental error.

A mixture of 50% helium and 50% nitrogen pre-cooled to 115 K was released from model tank—dike systems by Meroney et al., to simulate equivalent LNG spill behavior [27]. There was no guarantee that these experiments reproduced quantitatively similar situations in the field. Rather it was expected that the gross influences of different heat transfer conditions could be determined. Since the turbulence characteristics of the flow are dominated by roughness, upstream wind profile shape, and stratification, one expects the Stanton number in the field will equal that in the model, and heat transfer rates in the two cases should be in proper relation to plume entrainment rates. On the other hand, if temperature differences are such that free convection heat transfer conditions dominate, scaling inequalities may exist; nonetheless, model dispersion rates would be conservative.

Visualization experiments performed with equivalent dense isothermal and dense cold plumes revealed no apparent change in plume geometry. Concentration data followed similar trends in both situations. No significant differentiation appeared between insulated versus heat conducting ground surfaces or neutral versus stratified approach flows.

5.4 Dense gas plume interaction with surface features and buildings

Measurements of dense gas dispersion downwind of isolated releases have resulted in the development of many predictive models. The variation of such predictions is significant in assessing credibility of potential hazards, yet this uncertainty may well increase when the perturbations of building or structural aerodynamics are considered [37].

Dense plumes emitted from short stacks rising above cubical model buildings were found to avoid significant entrainment or wake effects when ejection velocities were greater than wind speed at stack height, and stack height exceeded twice the building height [15]. A criterion appropriate to ensure that the dense plume does not fall back into the recirculating cavity region would be $\bar{x}/d_0 \geqslant 3h_b/d_0$.

Model tests have been conducted to evaluate the rate of dispersion and extent of downwind hazards associated with the rupture of large LNG storage tanks [27]. Tank facilities considered include a low dike configuration (73 m diameter, 39 m tank surrounded by a 6.6 m dike 93 m by 100 m in area) and a high dike configuration (73 m diameter, 39 m tank surrounded by a concentric 81 m diameter dike 24 m tall). Dense plumes fell rapidly down over the dike walls to the ground and proceeded downwind in an undulating wave-like motion until the atmospheric turbulence started to penetrate and produce increased vertical dispersion. Figures 10 and 11 give

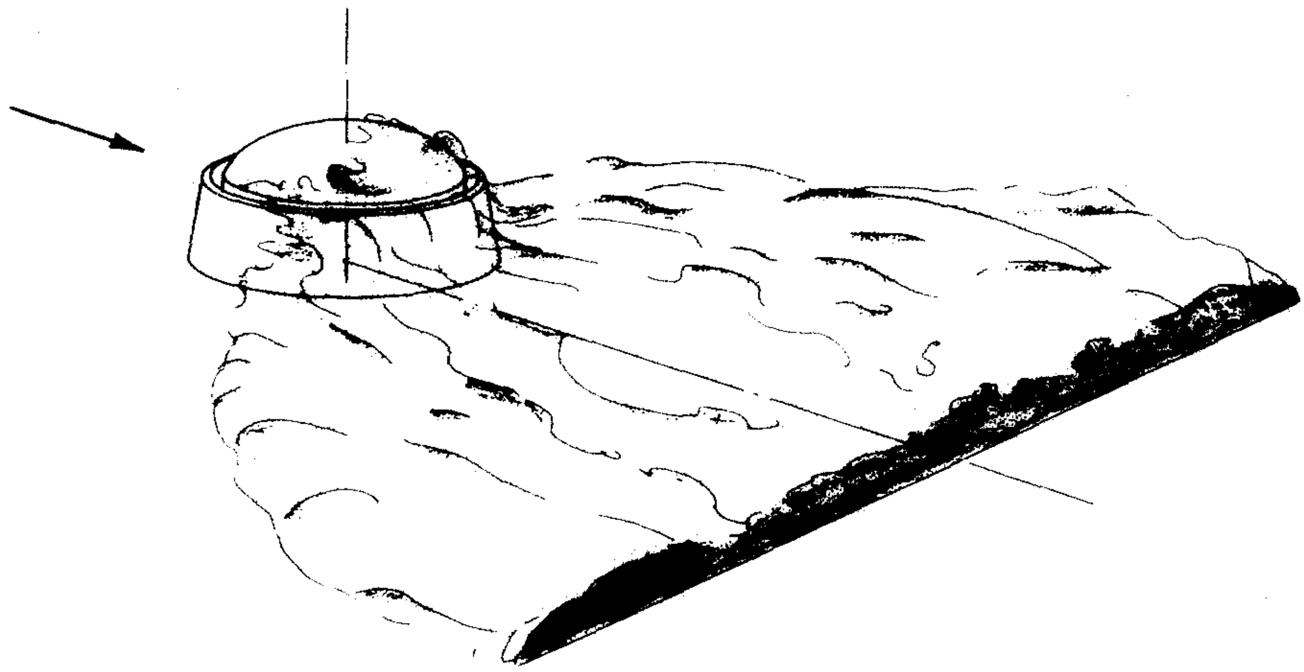

Fig. 10. Dense plume behavior downwind of a high dike/tank model.

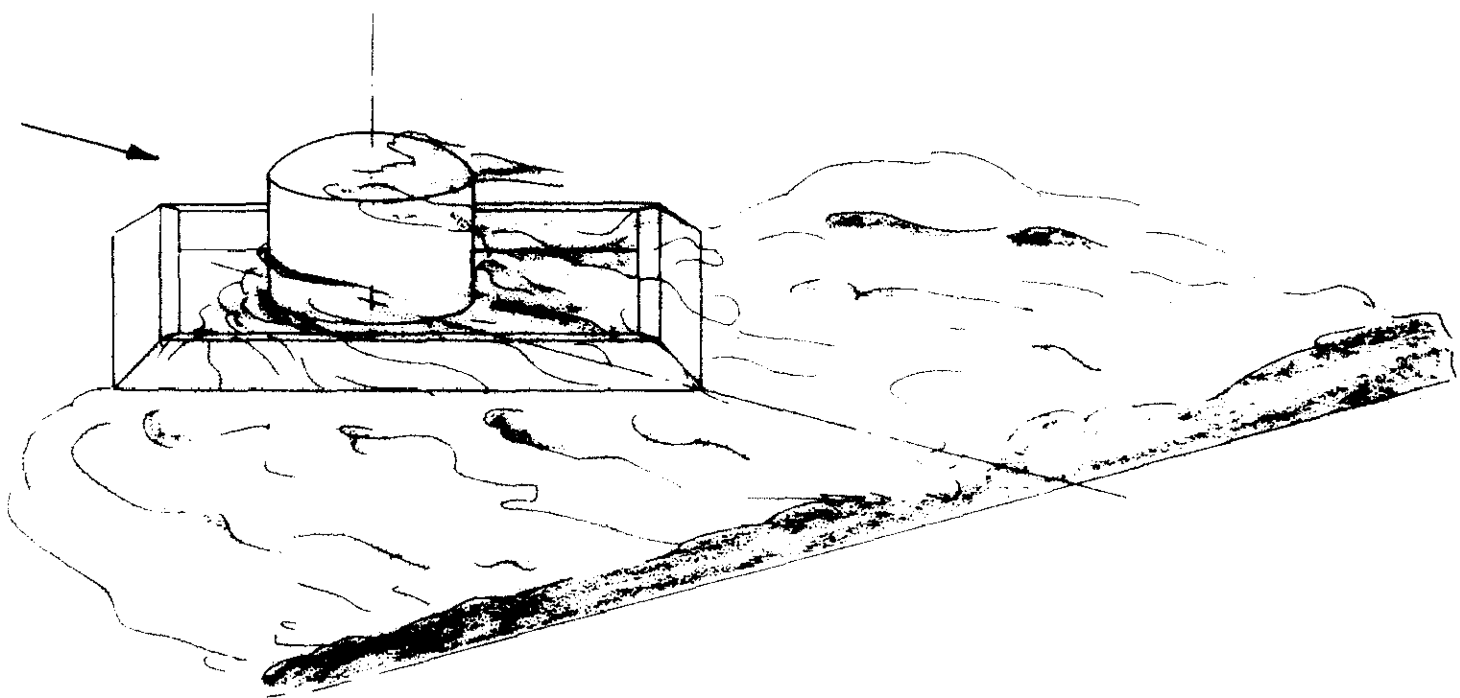

Fig. 11. Dense plume behavior downwind of a low dike/tank model.

an artist's representation of these flows for the high dike and low dike at 45°.

For the same dike geometry the rate of initial plume spread in the lateral directions varied directly with boil-off rate and inversely with wind speed. That is, to maintain approximately the same rate of spread with an increased boil-off, the wind speed would have to be increased and vice versa. At low wind speeds and high boil-off rates, the gravity spread rate increases to a point where the plume would spread out to the walls of the tunnel and then crawl upwind of the dike complex in a front perpendicular to the wind direction. With stable stratification the plume would spread out on the ground and migrate quite far upwind (300 meters) for the higher boil-off rates and low wind speeds. This upwind movement was present to some extent for the lower boil-offs and higher wind speeds.

The observed effects of the wake and cavity regions generated by the aerodynamics of the tank and dike structure varied with tank and dike geometry, wind speed, and stratification. For the Low Dike and Tank complex the effect of increased plume dispersion due to turbulence in its wake was insignificant. The only aerodynamic effect noticeable for this structure was that of a standing plume in the cavity regions of the tank and dike. For the high dike and tank, the effect of increased plume dispersion due to turbulence in its wake was most significant. Strong vortices which formed near the ground on each side of the dike structure would entrain a large amount of the plume and transport it downwind. This effect would give the plume a bifurcated form on the ground with what appears to be maximum concentration travelling downwind at a separation distance slightly greater than that of the dike diameter. Another vortex was generated on the tank top and travelled slightly upward in the downwind direction. This vortex appeared to act as a vent to the standing plume in the cavity region.

Concentration measurements were obtained for as many as 50 different sample points distributed over an equivalent ground zone of 100 to 200 meters long by 250 meters wide and in the vertical over a height of 0 to 120 meters. A series of vertical profiles revealed the shallow layer character of a dense gas plume. Ground-level contour plots of percent methane confirmed the presence of a bifurcated plume as suggested by the visualization photographs.

Even in the presence of the tank/dike wakes, the decay of maximum downwind concentrations fell only slightly below values predicted by the Battelle Columbus Laboratories (BCL) correlation, which represents an upper bound of all concentrations resulting from confined LNG land spills during the AGA phase II program, i.e.

$$\frac{C_{\max}\,\bar{u}\,L^2}{Q} \simeq 130\left(\frac{x}{L}\right)^{-2}, \tag{13}$$

where L is some characteristic length scale, Q is a maximum volumetric release rate, and u is the wind speed at an elevation of 10 m.

Dirkmaat studied the effect of a 50 m long, 21 m wide, 17.5 m obstacle placed at various locations near a modelled sudden guillotine fracture of an LPG pipeline [38]. A release of 1000 kg/sec of LPG during 6 minutes was simulated. On average the plume spread in a streamwise direction and the maximum contour areas tended to decrease compared to the undisturbed situation. Although the cloud contours were capriciously affected by the obstacle, the overall effect on cloud dimensions was not dramatic. Little could be said, however, about more complicated obstacle arrangements.

Terrain undulations can act to accelerate or depress dense gas dispersion. Hall and Meroney et al. report extensive upwind motion for dense gases released on modest ground slope [23,27]. The presence of upwind obstacles tends to lessen the effects of ground slope when surface layer turbulence is enhanced [27]. Studies of simulated spills of 6 cubic meter LNG volumes on a pond suggest that slight hill slopes (1:10) can detour dense plumes and reduce longitudinal distances to the lower flammability limit. Shallow valleys or gorges channel the plume and sustain high concentrations [14].

6.0 Conclusions

Wind tunnels have simulated a wide range of conditions associated with dense gas transport and dispersion. Scaling criteria suggest that existing facilities can simulate a wide range of release situations. Measurements of dense fluid behavior in both air and water facilities appear reproducible and consistent. Idealized release configurations appear optimal for testing and tuning numerical or analytical models. Wind tunnels are primarily limited by operational constraints associated with the necessary low wind speeds and low Reynolds numbers. Further effort is needed to quantify fully the effects of non-adiabatic heat transfer and humidity on cold plume model behavior.

Acknowledgments

The author gratefully acknowledges the support of the Gas Research Institute provided through Contract No. 5014-352-0203.

References

1 Liquified gaseous fuels safety and environmental control assessment program: A status report, U.S. Department of Energy, DOE/EV-0036, May 1979.
2 Recommended research on LNG safety, U.S. Department of Energy, DOE/EV-10024-1, March 1981.
3 J.D. Reid, Dispersion of denser-than-air gases, Report AQRB-80-005-L, Atmospheric Environment Service, Ontario, Canada, p. 24.
4 S.J. Kline, Similitude and Approximation Theory, McGraw-Hill Book Co., New York, 1965.
5 W.H. Snyder, Guidelines for fluid modeling of atmospheric diffusion, U.S. Environmental Protection Agency, Report EPA-600/8-81-009 (1981) p. 185.
6 R.N. Meroney, D.E. Neff, and J.E. Cermak, Wind-tunnel modeling of LNG spills, Proceedings AGA Transmission Conference, Montreal, Canada, May 8—10, 1978, T217—T223.
7 R.N. Meroney and D.E. Neff, Laboratory simulation of liquid natural gas vapor dispersion over land or water, in: Wind Engineering, Vol. 2, Pergamon Press, New York, 1980, pp. 1139—1150.
8 F.H. Chaudhry and R.N. Meroney, A laboratory study of diffusion in a stably stratified flow, Atm. Env., 74 (1973) 443.
9 J.E. Martin, The correlation of wind tunnel and field measurements of gas diffusion using Kr-85 as a tracer, Ph.D. Thesis, MMPP 272, University of Michigan, 1965.
10 N. Isyumov, T. Jondali, and A.G. Davenport, Model studies and the prediction of full-scale levels of stack gas concentration, J. of APCA, 26(10) (1976) 956.

11 K.M. Kothari, R.N. Meroney, and R.J. Bouwmeester, An algorithm to estimate field concentrations in the wake of power plant complexes under nonsteady meteorological conditions from wind-tunnel experiments, J. of Applied Meteorology, 20 (8) (1981) 934—943.
12 J.C. Yingst, R.N. Swanson, M.L. Mooney, J.E. Cermak and R.A. Peterson, Review of five wind-tunnel modeling results in complex terrain, 5th Symp. on Turbulence, Diffusion, and Air Pollution, Atlanta, Georgia, 1981, p. 148.
13 J.C. Weil, J.E. Cermak, and R.L. Petersen, Plume dispersion about the windward side of a hill at short range: Wind tunnel versus field measurements, 5th Symp. on Turbulence, Diffusion, and Air Pollution, Atlanta, Georgia, 1981, p. 159.
14 D.E. Neff and R.N. Meroney, Dispersion of vapor from LNG spills — Simulation in a meteorological wind tunnel of spills at China Lake Naval Weapons Center, California, Fluid Mechanics and Wind Engineering Report CER78-79DEN-RNM41, Colorado State University, Fort Collins, 1979, p. 77.
15 T.G. Hoot and R.N. Meroney, The behavior of negatively buoyant stack gases, 67th Annual Meeting of APCA, Denver, Colorado, Paper 74-210, 1974, p. 20.
16 F.T. Bodurtha, Jr., The behavior of dense stack gases, J. of APCA, 11 (9) (1961) 431—437.
17 A.P. Van Ulden, On the spreading of a heavy gas released near the ground, Loss Prevention and Safety Prevention Seminar, Delft, Netherlands, 1974.
18 G.J. Boyle and A. Kneebone, Laboratory investigations into the characteristics of LNG spills on water, evaporation, spreading and vapor dispersion, Shell Research Ltd., Report to API, 1972.
19 N. Isyumov and H. Tanaka, Wind-tunnel modeling of stack gas dispersion — Difficulties and approximations, in: Wind Engineering, Vol. II, Pergamon Press, New York, 1980, pp. 987—1002.
20 G.T. Skinner and G.R. Ludwig, Physical modeling of dispersion in the atmospheric boundary layer, Calspan Advanced Technology Center, Carmel, New York, Calspan Report No. 201, 1978.
21 K.M. Kothari and R.N. Meroney, Building effects on National Transonic Facility exhaust plume, Fluid Mechanics and Wind Engineering Report CER79-80KMK-RNM35, Colorado State University, Fort Collins, Colorado, 1979, p. 43.
22 R.S. Scorer, The behavior of chimney plumes, Int. J. Air Pollut., 1 (1959) 198—220.
23 D.J. Hall, C.F. Barrett, and M.O. Ralph, Experiments on a model of an escape of heavy gas, Warren Springs Laboratory Report LR 217 (AP), Dept. of Trade and Industry, United Kingdom, 1974, p. 25.
24 D.J. Hall, Further experiments on a model of an escape of heavy gas, Warren Springs Laboratory Report LR (312) AP, Dept. of Trade and Industry, United Kingdom, 1979, p. 47.
25 R.N. Meroney, D.E. Neff, and K.M. Kothari, Behavior of LNG vapor clouds: Tests to define the size, shape and structure of LNG vapor clouds: Annual Report for 1979—1980, Gas Research Institute Report GRI 79/0073, Chicago, Illinois, 1980.
26 R. Britter, The ground-level extent of a negatively buoyant plume in a turbulent boundary layer, Atm. Env. 147 (1980) 779—785.
27 R & D Associates and Colorado State University, Liquified natural gas wind-tunnel simulation and instrumentation assessments, U.S. Dept. of Energy Report SAN/W1364-01, 1978, p. 390.
28 R.G. Picknett, Field experiments on the behavior of dense clouds: Part 1, Main report, Report Ptn IL 1154/78/1, Chemical Defence Establishment, Porton Down, Gt. Britain, 1978, p. 93.
29 R.P. Koopman, B.R. Bowman, and D.L. Ermak, Data and calculations of dispersion on 5 m^3 LNG spill tests, Report UCRL-52876, Lawrence Livermore Laboratory, California, 1979, p. 31.

30 R.N. Meroney and D.E. Neff, Dispersion of vapor from LNG spills — simulation in a meteorological wind tunnel: Six cubic meter China Lake Spill Series, Proceedings of 4th Colloquium on Industrial Aerodynamics, Achen, F.R.G., June 18—20, 1980, pp. 303—320.
31 A. Lohmeyer, R.N. Meroney, and E.J. Plate, Model investigations on the spreading of heavy gases released from an instantaneous volume source at the ground, Proceedings of 11th NATO/CCMS Int. Tech. Mtg. on Air Pollution Modeling and Its Applications, Amsterdam, Netherlands, November 25—28, 1980, p. 15.
32 J.A. Fay, Gravitational spread and dilution of heavy vapor clouds, Proceedings of 2nd Intl. Symp. on Stratified Flows, Trondheim, Norway, June 24—27, 1980, pp. 471—494.
33 J.E. Simpson and R.E. Britter, The dynamics of the head of a gravity current advancing over a horizontal surface, J. Fluid Mech., 94 (1979) 477—495.
34 A.E. Germeles and E.M. Drake, Gravity spreading and atmospheric dispersion of LNG vapor clouds, Proceedings of 4th Intl. Symp. on Transport of Hazardous Cargoes by Sea and Inland Waterway, Jacksonville, Florida, 1975, pp. 519—539.
35 B.T. Yang and R.N. Meroney, Construction of a Lagrangian similarity distribution function for a non-stationary atmospheric diffusion process, Proceedings of 3rd AMS Conf. on Probability and Statistics in Atmospheric Science, Boulder, Colorado, June 19—22, 1973, p. 6.
36 J. Havens, Predictability of LNG vapor dispersion from catastrophic spills onto water: An assessment, U.S. Coast Guard, Dept. of Transportation, Report CG-M-09-87, 1977, p. 211.
37 R.N. Meroney, Turbulent diffusion near buildings, in: E. Plate (Ed.), Engineering Meteorology, Elsevier, 1982, pp. 481—525.
38 J.J. Dirkmaat, Experimental studies on the dispersion of heavy gases in the vicinity of structures and buildings, Proceedings of Symposium — Designing with the Wind, Nantes, France, Centre Scientifique et Technique du Baitment, June 15—19, 1981, pp. III-3-1 to III-3-13.
39 J. Sakagami and M. Kato, Diffusion and vapour rise of methane vapour from a real source in air stream, Natural Science Report of Ochanomizu University, Japan, 19 (2) 59—66.